CH), 144.0 (s; CH), 152.8 (s; CH), 157.5 (s; CH), 212.2 (s; CPd); IR (KBr): $\tilde{\nu}$ = 1637mb, 1450m, 1422s, 1384m, 1263s, 1225w, 1158m, 1033s, 860w, 772m, 637s, 549m, 519m cm^{-1}; FAB-MS (NBA): *m*/*z* (%): 727 (10) [M^+ – OTf+4H], 574 (90) [$M^+ - 2$OTf+H], 262 (100) [bipyPd$^+$].

Deprotonation of **6**: 1) A solution of **6** (193 mg, 0.63 mmol) in THF (5 mL) was added dropwise to a solution of KO*t*Bu (71 mg, 0.63 mmol) in THF (10 mL) at −78 °C. The solution was then evaporated to dryness and the residue was separated by chromatography on silica gel (CH_2Cl_2:ethyl acetate 4:1). Yields: 34 mg **7** (34%), 37 mg **5** (37%). 2) KO*t*Bu (58 mg, 0.52 mmol) was added slowly to a solution of **6** (160 mg, 0.52 mmol) in THF (10 mL) at −78°C. The solution was then evaporated to dryness and the residue separated by chromatography on silica gel (CH_2Cl_2:ethyl acetate 4:1). Yield: **7** (70 mg, 86.2%). Compounds **5** and **7** have been described in the literature and could be unambiguously identified by spectroscopic data (EI-MS, ESR, and UV measurements).[9, 10]

Received: August 1, 2001 [Z17648]

[1] a) R. Weiss, S. Reichel, M. Handke, F. Hampel, *Angew. Chem.* **1998**, *110*, 352 – 354; *Angew. Chem. Int. Ed.* **1998**, *37*, 344 – 347; b) R. Weiss, S. Reichel, *Eur. J. Inorg. Chem.* **2000**, 1935 – 1939.

[2] K. Deuchert, S. Hünig, *Angew. Chem.* **1978**, *90*, 927 – 938; *Angew. Chem. Int. Ed. Engl.* **1978**, *12*, 875 – 886.

[3] S. Reichel, Dissertation, Universität Erlangen-Nürnberg, **1998**.

[4] The conceivable, still more electrophilic oxidation products SEM/OX and OX/OX are not addressed in the following discussion.

[5] R. Weiss, N. Kraut, F. Hampel, *J. Organomet. Chem.* **2001**, *617*, 473 – 482.

[6] a) A. Caneschi, D. Gatteschi, N. Lalioti, C. Sangregorio, R. Sessoli, G. Venturi, A. Vindigni, A. Rettori, M. G. Pini, M. A. Novak, *Angew. Chem.* **2001**, *113*, 1810 – 1813; *Angew. Chem. Int. Ed.* **2001**, *40*, 1760 – 1763; b) S. Pillet, M. Souhassou, Y. Pontillon, A. Caneschi, P. Gatteschi, C. Leconte, *New J. Chem.* **2001**, *25*, 131 – 143.

[7] a) E. F. Ullman, J. H. Osiecki, D. G. B. Boocock, R. Darcy, *J. Am. Chem. Soc.* **1972**, *94*, 7049 – 7059; b) A. Caneschi, J. Laugier, P. Ray, *J. Chem. Soc. Perkin Trans. 1* **1987**, 1077 – 1079.

[8] This will be reported elsewhere.

[9] D. G. B. Boocock, R. Darcy, E. F. Ullman, *J. Am. Chem. Soc.* **1968**, *90*, 5945 – 5946.

[10] E. F. Ullman, D. G. B. Boocock, *J. Chem. Soc. Chem. Commun.* **1969**, *20*, 1161 – 1162.

[11] The conventional triplet compound with σ – π configuration can be ignored here because the single n electron pair on C2 is not only highly stabilized by ring-strain effects but also inductively and hyperconjugatively by the NO group.[12]

[12] R. Weiss, N. Kraut, T. Clark, N. J. R. Eikema Hommes, R. Puchta, unpublished results.

[13] In a control experiment it was demonstrated that **5** is not formed simply by the reduction of **6** by the base: if the corresponding C2-deuterated salt is used instead of **6**, in addition to the dimer **7**, the radical **5** is obtained by inverse base addition. (MS analysis).

[14] a) A. J. Arduengo, J. R. Goerlich, W. J. Marshall, *Liebigs Ann.* **1997**, 365; b) R. W. Alder, M. E. Blake, *Chem. Commun.* **1997**, 1513.

[15] a) D. Enders, H. Gielen, G. Raabe, J. Runsink, J. H. Teles, *Chem. Ber.* **1996**, *129*, 1483 – 1488; b) W. A. Herrmann, M. Elison, J. Fischer, C. Köcher, G. R. J. Artus, *Angew. Chem.* **1995**, *107*, 2602 – 2605; *Angew. Chem. Int. Ed. Engl.* **1995**, *34*, 2371 – 2374.

[16] Crystal structure data for **10**: $C_{26}H_{32}F_6N_6O_{10}PdS_2$, M_r = 873.10, monclinic, space group *C*2/*c*, *a* = 40.219(8), *b* = 7.5618(15), *c* = 23.737(5) Å, β = 108.16(3)°, *V* = 6859(2) Å^3, *Z* = 8, ρ_{calcd} = 1.691 Mg m^{-3}, crystal dimensions: 0.20 × 0.20 × 0.10 mm, $Mo_{K\alpha}$ radiation (λ = 0.71073 Å), *T* = 173(2) K, *F*(000) = 3536; the data were collected with a Nonius Kappa CCD Area Detector in the range of 2.13° < θ < 25.02°(11 453 reflections were measured, of which 6004 were independent and 4783 with $I > 2\sigma(I)$). The absorption correction was carried out with the program Scalepack (Z. Otwinowski, W. Minor, *Methods Enzymol.* **1997**, *276*, 307). The structure was solved by direct methods (SHELXS 97); structure refinement against F^2 (SHELXL 97). The hydrogen atoms were fixed at idealized positions (riding-model). Refinement *R* values: *R*1 = 0.0477 for $I > 2\sigma(I)$, *wR*2 = 0.1420 for all data. Residual electron density 1.665/ – 0.890 e Å^{-3}. Crystallographic data (excluding structure factors) for the structure reported in this paper have been deposited with the Cambridge Crystallographic Data Centre as supplementary publication no. CCDC-164924. Copies of the data can be obtained free of charge on application to CCDC, 12 Union Road, Cambridge CB2 1EZ, UK (fax: (+44) 1223-336-033; e-mail: deposit@ccdc.cam.ac.uk).

Visualization of Molecular Recognition Events on Microstructured Lipid-Membrane Compartments by In Situ Scanning Force Microscopy**

Stephanie Künneke and Andreas Janshoff*

Cell membranes are the most important interfaces in biological systems. A variety of reactions, such as molecular biorecognition of soluble proteins by receptor lipids, take place at this unique surface. Artificial solid-supported lipid bilayers are well suited model systems that allow the study of certain reactions under defined quasi-native conditions. Additionally, they enable the assembly of biosensor surfaces with ordered receptor molecules in a densely packed matrix efficiently suppressing nonspecific adsorption of biomolecules.[1]

Arrays of microstructured individually addressable lipid-membrane compartments meet the requirements given by analytical applications, combinatorial libraries, or pharmacological screening, which create a demand for high-throughput analysis and highly comparable and reliable results.[2] A structured surface that enables a direct comparability of biomaterials and a parallel analysis of protein – receptor interactions on different membranes or receptors under identical ambient conditions is well suited if not required especially for scanning force microscopy of material contrasts and visualization of lipid – protein interactions. Because lipid membranes rarely show topographical features, a microstructured lipid bilayer with defined boundaries becomes necessary to compare contrasts qualitatively and to enable parallel control measurements. While the structuring of proteins and nucleic acids is relatively straightforward, the preparation and structuring of lipid bilayers requires handling in aqueous solution.

Methods based on contact printing for structuring lipid membranes are limited to a very small number of different lipid compositions, moreover the individual addressibility of the segments is cumbersome.[3]

We have developed a general microstructuring procedure for generating numerous selectively functionalized lipid-

[*] Prof. Dr. A. Janshoff, S. Künneke
Johannes Gutenberg Universität Mainz
Institut für Physikalische Chemie
Jakob Welder Weg 11, 55128 Mainz (Germany)
Fax: (+49) 6131-39-22970
E-mail: janshoff@mail.uni-mainz.de

[**] This work was supported by the Deutsche Forschungsgemeinschaft (JA 963/1-2).

  1433-7851/02/4102-0314 $ 17.50+.50/0

membrane compartments on a solid support in close vicinity to each other. The number of different lipid segments is presently only limited to the handling of the manual injection of vesicle solutions.[4]

The manufacturing of an array of solid-supported lipid bilayers in the micrometer regime is accomplished by a combination of vesicle spreading[5] and the formation of a microfluidic network (μFN).[6]

The technique of material molding in capillaries formed by elastomers was first established by Whitesides et al.[6] The basic idea of this technique, which belongs to the family of soft lithography, is to create a structured elastomer that functions as the mold, which provides a hydrodynamically coupled network of empty channels once brought into contact with the substrate. The structure of the mold is obtained by curing the two components of the polydimethylsiloxane (PDMS) on a coated silicon wafer, which displays the inverse master structure, and subsequent removal of the PDMS-replicate from the silicon wafer. Prior to use it is necessary to expose the PDMS mold to an O_2 plasma to render the surface hydrophilic and hence provide a temporal seal between the mold and the glass substrate.[7] As a consequence, the capillaries are filled rapidly with vesicle suspensions due to the high surface tension of the capillary walls. Delamarche et al. used this method successfully for microstructuring of proteins.[8]

Figure 1 illustrates schematically the microstructuring process of solid-supported membrane segments.[4, 9] The flow pads are filled individually with different vesicle solutions through small preformed holes from the top of the PDMS

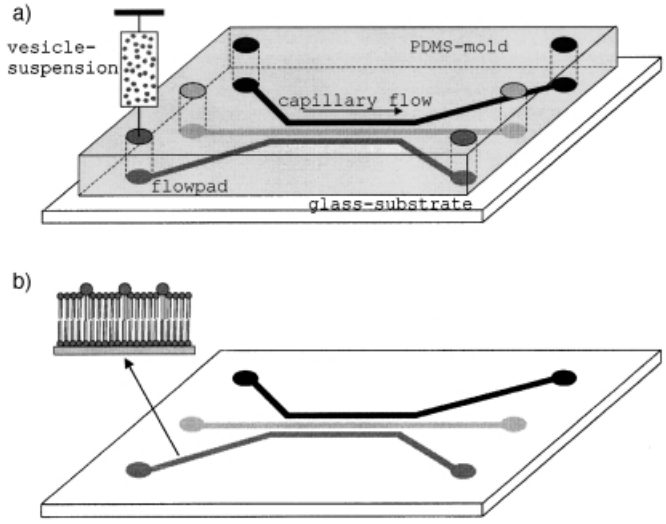

Figure 1. Schematic representation of the microstructuring of solid-supported membrane segments of different compositions.

mold. The empty channels are filled rapidly with the injected vesicle-suspension in a laminar fashion. The liposomes adhere on the glass surface and subsequently spread onto the interfaces forming planar lipid bilayers (Figure 1a). After removal of the PDMS mold and immediate rinsing of the sample with excess buffer, the separated lipid–membrane compartments remaining on the substrate (Figure 1b) are readily accessible to optical techniques and high-resolution surface analysis tools.

To demonstrate the suitability of this method we first focus on optical investigations of the specific protein–receptor interaction of the tumor-marking protein peanut agglutinin (PNA) from *Arachis hypogaea* on lipid-membrane segments of 1,2-dimyristoyl-*sn*-glycero-3-phosphocholine (DMPC) without any receptor molecules and DMPC with the receptor ganglioside asialo-G_{M1}[10] incorporated in a membrane segment using confocal laser scanning microscopy. Additionally, the specific binding of cholera toxin B-oligomer[11] (CTB) to the receptor ganglioside G_{M1} embedded in a DMPC-membrane segment was investigated by scanning force microscopy.

Specific recognition of saccharide structures on cell surfaces, which is shown here using these two prominent examples, is a relevant issue for the differentiation of normal and malign cell types, for the binding of toxic proteins such as cholera, pertussis, botulinum, tetanus, and diphtera toxin as well as for inflammatory processes.

Figure 2 shows the fluorescence microscopic images of two lipid–membrane segments consisting of DMPC doped with 4 mol% of the receptor asialo-G_{M1} and 1 mol% of

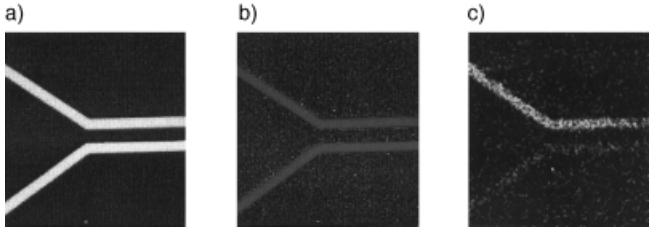

Figure 2. Fluorescence microscopy images of two DMPC/β-Bodipy-500/510-C_{12} HPC segments (upper segment contains the receptor asialo-G_{M1}) before (a,b) and after (c) addition of 278 nM TRITC-x-PNA. a) Fluorescein-fluorescence; b, c) rhodamin-fluorescence.

the fluorophore β-Bodipy-500/510-C_{12}HPC (upper segment; β-Bodipy-500/510-C_{12}HPC = 2-(4,4-difluoro-5-methyl-4-bora-3a,4a-diaza-*s*-indacene-3-dodecanoyl)-1-hexadecanoyl-*sn*-glycero-3-phosphocholine) and DMPC with 1 mol% β-Bodipy-500/510-C_{12} HPC (lower segment) in the fluorescein fluorescence (Figure 2a) before adding the protein. Figure 2b shows the control experiment with rhodamine fluorescence. The specific binding of the lectin tetramethylrhodamine-B isothiocyanate(TRITC)-x-peanut agglutinin (TRITC-x-PNA) to the membrane segment containing asialo-G_{M1} (upper segment in Figure 2c) is accompanied by an increase of the rhodamine fluorescence intensity after incubating a 278 nM protein solution for 10 min.

Compared to fluorescence microscopy and other optical methods, scanning force microscopy is advantageous for the analysis of protein–lipid interactions because the protein binding can be directly imaged by the height change without labeling techniques, and additionally, imaging of single proteins is possible.

Figure 3a–c display SFM topography images of DMPC/G_{M1} and DMPC lipid segments on a glass substrate before (Figure 3a) and after (Figure 3b, c) addition of 2.7 nM CTB. Histogram analysis (Figure 3d) was performed by using

  1433-7851/02/4102-0315 $ 17.50+.50/0

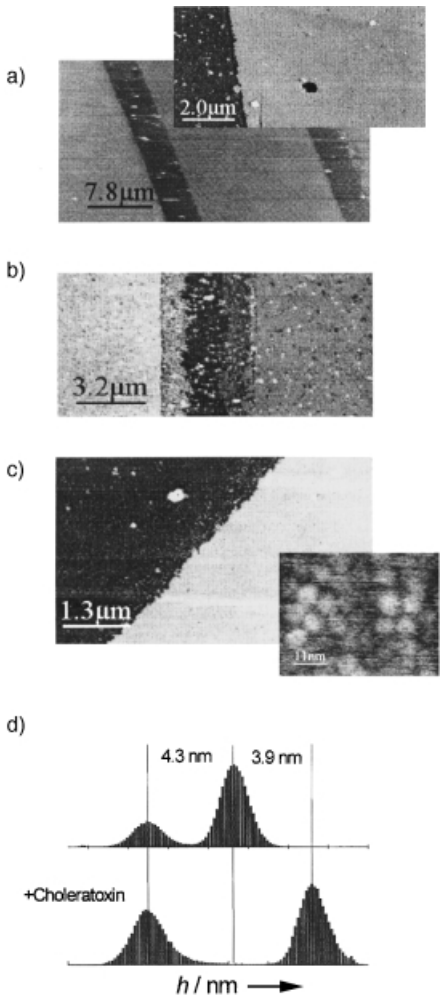

Figure 3. Scanning force microscopy images (tapping-mode, total height 14 nm) showing the topography of different lipid membrane segments on a glass substrate (a) before and (b,c) after addition of 2.7 nM CTB. The lipid segment on the left-hand side of b) consisting of DMPC/GM_1 is covered with cholera toxin homogeneously, while the segment on the right side lacks receptor lipids and shows no sign of protein adsorption after addition of CTB. The average increase in height was 3.9 nm (d) after the addition of CTB. The inset in c) (deflection signal, contact-mode) shows individual B-oligomers providing the ultimate proof that CTB is adsorbed on the surface (lipid segment).

Figure 3a (portrait figure) and Figure 3c. The average height of substrate and membrane was determined by fitting Gauss functions to the data. The average height difference between the substrate and the DMPC/G_{M1} membrane is 4.3 nm before addition of the protein and 8.2 nm after the incubation of CTB (Figure 3d). The specific binding of the proteins was revealed by the integral measurement of the height, and confirmed by resolving single molecules, namely CTB (inset in Figure 3c).[12] The applicability of the presented lipid array for investigation of specific binding of biomaterials is demonstrated by the absence of both height change and protein structure of the DMPC membrane segment without receptor, which is not possible by fluorescence measurement alone (right segment in Figure 3b).

The combination of this preparatively simple method with scanning force microscopy is particularly interesting, since here not only molecular recognition for biosensor applications is used, but also the theoretical basis of material properties, such as adhesion contrast, viscoelasticity of different lipids, and receptor organization in membranes, could be investigated on a single structured surface.

Experimental Section

Small unilamellar vesicles of 1,2-dimyristoyl-*sn*-glycero-3-phosphocholine (DMPC: Avanti Polar Lipids, Alabaster, Al, USA) doped with 2 mol% GM_1 or 4 mol% asialo-G_{M1} (Sigma, Dreieich, Germany), and 1 mol% β-Bodipy-500/510-C_{12}HPC (Molecular Probes, Eugene, OR, USA) were prepared by the extrusion method using two stacked polycarbonate membranes (average pore diameter 50 nm) und subsequent sonification.

The B-oligomer of the cholera toxin (*Vibrio cholerae*) was purchased from CalBioChem (La Jolla, CA, USA), the fluorophore-labeled protein tetramethylrhodamine-isothiocyanate(TRITC)-x-peanut agglutinin (*Arachis hypogaea*) was obtained from Sigma (Dreieich, Germany).

A commercial atomic force microscope AFM (Bioscope with Nanoscope IIIa controller, Veeco Digital Instruments) with lipid cell and silicon nitride cantilevers that exhibit a nominal spring constant of 0.12 $N m^{-1}$ (tapping-mode) and 0.06 $N m^{-1}$ (contact-mode) was used for the atomic force microscopy (AFM) experiments. The scan rates were set to 0.5 Hz in tapping-mode and 4 Hz in contact mode for recording the deflection signal.

Confocal laser scanning microscopy was performed by using a MRC 600 (Bio-Rad, München, Germany).

All experiments were performed in a pH 7.4 buffer from 10 mM (tris(hydroxymethyl)aminomethane(Tris)/HCl and 100 mM NaCl.

A 10:1 mixture of the elastomer and curing agent of polydimethylsiloxane PDMS (Sylgard 184, Dow Corning Silicon Elastomer, West Midlands) was cured on a structured silicon wafer (IMSAS, Bremen, Germany) which had been coated with a thin film of 1*H*,1*H*,2*H*,2*H*-perfluorodecyldimethylchlorosilane prior to use.

The capillary structures used in these experiments are 15 μm wide, 3 μm high, and 2 mm long. The five parallel capillaries are separated from each other by a distance of 5 μm ending on either side in flow pads of 2.13 × 2.13 mm. The PDMS-replicates are used up to 50 times. There are 0.1 μL of vesicle solution injected in each flow pad.

Received: August 9, 2001 [Z17696]

[1] E. Sackmann, *Science* **1996**, *271*, 43 – 48.
[2] S. Fodor, J. L. Read, M. C. Pirrung, L. Stryer, A. T. Lu, D. Solas, *Science* **1991**, *251*, 767 – 773.
[3] a) L. A. Kung, L. Kam, J. S. Hovis, S. G. Boxer, *Langmuir* **2000**, *16*, 6773 – 6776; b) J. S. Hovis, S. G. Boxer, *Langmuir* **2000**, *16*, 894 – 897; c) K. Morigaki, T. Baumgart, A. Offenhäusser, W. Knoll, *Angew. Chem.* **2001**, *113*, 184 – 186; *Angew. Chem. Int. Ed.* **2001**, *40*, 172 – 174.
[4] A. Janshoff, S. Künneke, *Eur. Biophys. J.* **2000**, *29*, 549 – 554.
[5] A. A. Brian, H. M. McConnell, *Proc. Natl. Acad. Sci USA* **1984**, *81*, 6159 – 6165.
[6] a) "Soft lithography": Y. Xia, G. M. Whitesides, *Annu. Rev. Mater. Sci.* **1998**, *28*, 153 – 184; b) E. Kim, Y. Xia, G. M. Whitesides, *J. Am. Chem. Soc.* **1996**, *118*, 5722 – 5731.
[7] a) E. Delamarche, A. Bernard, H. Schmid, B. Michel, H. Biebuyck, *Science* **1997**, *276*, 779 – 781; b) A. Papra, A. Bernard, D. Juncker, N. Larsen, B. Michel, E. Delamarche, *Langmuir* **2001**, *17*, 4090 – 4095.
[8] E. Delamarche, A. Bernard, H. Schmid, A. Bietsch, B. Michel, H. Biebuyck, *J. Am. Chem. Soc.* **1998**, *120*, 500 – 508.
[9] For clarity there are only three parallel channels presented which are marked with diferent gray scales.
[10] A. Janshoff, C. Steinem, M. Sieber, H.-J. Galla, *Eur. Biophys. J.* **1996**, *25*, 105 – 113.
[11] a) J. X. Mou, J. Yang, Z. F. Shao, *J. Mol. Biol.* **1995**, *248*, 507 – 512; b) A. K. Singh, S. H. Harrison, J. S. Schoeniger, *Anal. Chem.* **2000**, *72*, 6019 – 6024.
[12] The height of the CTB determined by X-ray-diffraction is 3.5 nm. See:E. A. Merritt, P. Kuhn, S. Sarfaty, J. L. Erbe, R. K. Holmes, W. G. Hol, *J. Mol. Biol.* **1998**, *282*, 1043.

  1433-7851/02/4102-0316 $ 17.50+.50/0